Sādhanā (2024)49:218
https://doi.org/10.1007/s12046-024-02563-3

Analytical assessment of dynamic response of fiber-reinforced polymer laminate on concrete wall under blast loads

YASHWARDHAN PUSHKARAJ NAIKNIMBALKAR[1], SHAMSHER BAHADUR SINGH[2] and VASANT ANNASAHEB MATSAGAR[3,*]

[1]Multi-Hazard Protective Structures (MHPS) Laboratory, Department of Civil Engineering, Indian Institute of Technology (IIT) Delhi, Hauz Khas, New Delhi, India
[2]Department of Civil Engineering, Birla Institute of Technology and Science (BITS) Pilani, Pilani, Rajasthan, India
[3]Department of Civil Engineering, Indian Institute of Technology (IIT) Delhi, Hauz Khas, New Delhi, India
e-mail: ypnaiknimbalkar@gmail.com; sbsingh@pilani.bits-pilani.ac.in; matsagar@civil.iitd.ac.in

MS received 8 December 2023; revised 29 March 2024; accepted 3 May 2024

Abstract. Composite laminates are increasingly used for blast-resistant applications in structures owing to the rise of such fanatic activities. For the safe and economical design of blast-resistant structures, it is necessary to study the influence of various laminate characteristics on their dynamic behavior. Here, the influence of design parameters of fiber-reinforced polymer (FRP) laminates in mitigating the dynamic response of a concrete wall when subjected to surface blast loads has been studied. Furthermore, a generalized analytical approach employing classical laminate theory has been presented to analyze the dynamic behavior of a concrete wall applied with the FRP laminate(s) under various explosion-induced load scenarios. It is found that the stacking sequence of the laminae and the number of layers in the laminate decrease the response by about 5% and 15% among the considered configuration, respectively. Moreover, using the FRP laminates reduce the dynamic response of the concrete wall by 18%. Through a detailed parametric study, it has also been observed that the center node displacement of the wall decreases with an increase in standoff distance, an increase in the thickness of the concrete wall, and a decrease in charge weight.

Keywords. Analytical solution; dynamic response; blast; classical laminate theory; hamilton's principle; fiber-reinforced polymer (FRP).

1. Introduction

In recent times, there has been a significant increase in terrorist and unintentional explosions, such as the 2008 Mumbai attacks, the Beirut explosion in 2020, and many more. During these blast events, many injuries and casualties were caused by the fragmentation and collapse of structures. Thus, blast-resistant structures have become increasingly important in a wider context, apart from the military setups, like the transportation and oil refinery industries. These buildings can resist the force of an explosion and protect the people, property, and infrastructure inside them. The construction of blast-resistant structures requires a variety of hardening strategies, design principles, and building methods. Some of the most common design principles are increasing the explosion's standoff distance, e.g., perimeter protection, decreasing the combustible material within and around the structure, and using materials with high strength and ductility. However, it is vital to comprehend blast loads and structural response under such high strain rate loading to design blast-resistant structures.

Composite structures are increasingly used for enhancing blast resistance due to their high strength-to-weight ratio and excellent energy-absorbing properties. Composite fiberglass, carbon fiber, or aramid panels are renowned for their high strength-to-weight ratio. The overall strength and explosion resistance can be substantially enhanced by strengthening the existing concrete walls with composite panels. The composite panels are significantly lighter than the concrete walls. This enhances the strength of the structure and thus is an effective method to improve the blast resistance performance of new structures as well as of those not initially built for resisting blast loads, i.e., retrofit.

Early research on blast loading was carried out experimentally, mainly using Trinitrotoluene (TNT) explosives at particular standoff distances. Conducting several such field tests is a costly and time-consuming affair. Due to this, only

*For correspondence
Published online: 15 July 2024

a limited number of explosions could be conducted to obtain the results and study the results. The effectiveness of an externally reinforced concrete slab with fiber-reinforced polymer (FRP) was studied in [1] using an experimental setup, and it was found that the maximum displacement decreased by 25% with the external reinforcement. Series of explosive tests were conducted on a concrete wall strengthened with carbon FRP (CFRP), glass FRP (GFRP), and both using TNT, as reported in [2] and [3]. It was observed that the FRP laminate helped reduce not only the maximum displacement but also the spalling in the wall and fragmentation (splinters formation). Further, conclusions were challenging to draw from these studies due to the availability of a limited number of results.

Finite element analysis (FEA) later emerged as a valuable tool for analyzing various loading conditions and configurations. Yet, the computational cost and time required for FEA limit its applicability to analyze numerous configurations. Jain *et al* [4] conducted a study on the dynamic response of reinforced concrete walls under blast loading by using high-fidelity finite element analysis (FEA), describing the damage and deformations of the concrete wall and emphasizing the importance of understanding the dynamic response of concrete structures to enhance their resilience against blast-induced hazards. Such detailed FEA requires significantly high computational resources and time requirements, and for iterative design processes it poses practical limitations. Maazoun *et al* [5] analyzed reinforced concrete (RC) slabs retrofitted with carbon fiber-reinforced polymer (CFRP) strips under blast loading using finite element analysis. This study also reported the effect of the width and thickness of CFRP strips on the mitigation of the response. However, for arriving at preliminary design instead of the detailed nonlinear FEA simplified method is essential prior to undertaking modelling and analysis of the structures subjected to blast loading.

In 1984, Kingery and Bulmash also provided various semi-empirical relations [6], which helped overcome the limitation of results as researchers started using analytical methods to generalize the response, reducing reliance on conducting field tests. A review of several empirical relations to calculate blast wave parameters was provided in [7]. An analytical expression to determine the response of thick anti-symmetrically laminated angle-ply, simply supported plates to conventional blast loading was developed and reported in [8].

Based on the literature review, it is evident that finite element analysis (FEA) has proven to be a powerful tool to analyze a higher number of loading conditions and configurations than the experimental method, especially when conducting the experiments is a costly affair in case of structures exposed to blast loading and repeatability of the outcomes remains a concern. However, the inherent limitations of computationally rigorous FEA in analyzing all possible configurations underscore the need for a preliminary analytical method to assess the influence of various parameters on the structural response without employing extensive computational resources. The process of simplified analysis allows us to identify configurations with most desirable performance, which can then undergo further analysis using high-fidelity FEA to predict the behavior under blast-induced load and potential damage. Subsequently, the most suitable configuration can be determined based on these high-end analyses. To address this research gap, an analytical approach has been presented in this study by using the classical laminate theory and Hamilton's principle in conjunction to conduct a preliminary analysis of FRP laminate on a concrete wall and determine the dynamic response of the system under surface blast loads.

Previous studies further suggest that despite advancements in blast-resistant design and research, there has been limited exploration of the influence of design parameters of the FRP laminates, such as the laminate material, the number of lamina layers in the laminate, and the stacking sequence. In view of these challenges, various parametric sensitivity studies have been conducted in the present study to address this research gap and aid engineers in making preliminary design decisions regarding the configuration of the FRP laminates.

The main objectives of the present study are: (a) to present an analytical method that provides the dynamic response of an FRP laminate on a concrete wall subjected to surface blasts by considering the influence of several parameters, such as the type of explosive, the weight of the explosive, dimensions of the wall, and laminate configurations to assist engineers in making preliminary design decisions without using computationally costly methods such as nonlinear/ higher order finite element analysis; (b) to assess and compare the dynamic response of FRP laminated concrete walls subjected to surface blasts due to changes in the thickness of the concrete wall, stacking sequence, number of lamina layers in the laminate, and the FRP material.

2. Blast load calculations

An explosion causes sudden release of tremendous energy, which travels outward from the source of the explosion in the form of a wave. This blast wave causes an abrupt increase in air pressure followed by a rapid decrease of it, causing a shock wave that exerts tremendous dynamic force on the structure with which the blast wave interacts. This blast wave is dependent on the type of explosive, point (air, surface, etc.), and radial distance (R) from the source of the explosion [9]. The blast waveform is described through modified Friedlander's equation (Eq. 1). Kingery-Bulmash plots are used to determine incident overpressure (P_{so}), incident impulse (i_s), arrival time (t_a), and positive duration (t_o) [10]. The incident overpressure is higher in the

case of surface blasts due to reflection from the ground. Thus, peak reflected overpressure (P_r) is used instead of incident overpressure in the modified Friedlander's equation. The reflected overpressure is obtained using Eq. (2). Subsequently, Eqs. (3) and (4) have been used to calculate the scaled distance and equivalent weight of explosives (W_e).

$$P_s(t) = P_{so}\left(1 - \frac{t}{t_o}\right)e^{-b\frac{t}{t_o}}, \tag{1}$$

$$P_r = 2P_{so}\frac{4P_{so} + 7P_o}{P_{so} + 7P_o}, \tag{2}$$

$$Z = \frac{R}{\sqrt[3]{W_e}}, \tag{3}$$

$$W_e = W_{\exp}\frac{H^d_{\exp}}{H^d_{TNT}}, \tag{4}$$

Several relationships are available in the literature to determine the decay parameter (b) of a blast wave based on the scaled distance (Z). The variation in the decay parameter with standoff distance described by various researchers is expressed in [11]. In this study, blast wave parameters for the modified Friedlander's are obtained using the most extensively used report by Kingery and Bulmash and US military guidelines such as the Unified Facilities Criteria (UFC). Thus, to maintain uniformity in the blast wave parameters, the decay parameter obtained by Kingery and Bulmash, as described in [11], is used in this study.

For calculating the decay parameter b, the blast impulse is used iteratively, and the obtained values are fitted for various scaled distances and are expressed through the polynomial relationships in Eqs. (5a) and (5b) as given in [11].

$$Y = C_0 + C_1U + C_2U^2 + \cdots + C_nU^n, \tag{5a}$$

$$U = K_0 + K_1T, \tag{5b}$$

where, Y is the common logarithm of the decay coefficient, and T is the common logarithm of the scaled distance. The constants $\{K_0, K_1, C_0, C_1 \ldots C_n\}$ are defined through the least-squares fitting of the calculated decay coefficient values and have been provided for surface blasts for close-field ($0.4 < Z < 2.5$ m/kg$^{1/3}$) as well as far-field blasts ($2.5 < Z < 40$ m/kg$^{1/3}$) in [11].

3. Analytical formulations

An analytical model to determine the linear dynamic response of a simply-supported FRP laminated wall is presented here to reduce the computational cost involved in finite element simulations. The analytical modelling has been conducted and the resulting equations are solved using in-house MATLAB R2022b [12] code developed. The classical laminate theory is used for analyzing a FRP laminated concrete wall. As per the classical laminate theory, the displacement fields in terms of midplane displacements are given using Eqs. (6a)-(6c).

$$u(x,y,z,t) = u_0(x,y,t) - zw_{0,x}(x,y,t), \tag{6a}$$

$$v(x,y,z,t) = v_0(x,y,t) - zw_{0,y}(x,y,t), \tag{6b}$$

$$w(x,y,z,t) = w_0(x,y,t), \tag{6c}$$

where, $\partial w_0/\partial i$ is written as $w_{0,i}$.

The strain displacement relations are obtained in matrix form as given in Eqs. (7a), (7b),

$$\begin{Bmatrix}\varepsilon_{xx}\\ \varepsilon_{yy}\\ \gamma_{xy}\end{Bmatrix} = \begin{Bmatrix}u_{0,x}\\ v_{0,y}\\ u_{0,y} + v_{0,x}\end{Bmatrix} + z\begin{Bmatrix}-w_{0,xx}\\ -w_{0,yy}\\ -2w_{0,xy}\end{Bmatrix}, \tag{7a}$$

$$\begin{Bmatrix}\varepsilon_{xx}\\ \varepsilon_{yy}\\ \gamma_{xy}\end{Bmatrix} = \begin{Bmatrix}\varepsilon_{0xx}\\ \varepsilon_{0yy}\\ \gamma_{0xy}\end{Bmatrix} + z\begin{Bmatrix}\kappa_{xx}\\ \kappa_{yy}\\ \kappa_{xy}\end{Bmatrix}. \tag{7b}$$

The constitutive relations for an orthotropic material transformed to x-y coordinate system in terms of transformed reduced stiffness are given in Eq. (8),

$$\begin{Bmatrix}\sigma_{xx}\\ \sigma_{yy}\\ \tau_{xy}\end{Bmatrix}_k = \begin{bmatrix}\overline{Q}_{11} & \overline{Q}_{12} & \overline{Q}_{16}\\ \overline{Q}_{12} & \overline{Q}_{22} & \overline{Q}_{26}\\ \overline{Q}_{16} & \overline{Q}_{26} & \overline{Q}_{66}\end{bmatrix}_k \begin{Bmatrix}\varepsilon_{xx}\\ \varepsilon_{yy}\\ \gamma_{xy}\end{Bmatrix}_k. \tag{8}$$

Hamilton's principle is used to obtain the equilibrium relations of the laminated wall as per Eq. (9), where strain energy (U), kinetic energy (T), and work energy (E) are considered. The equilibrium relations in the form of resultant stresses (N_{xx}, N_{xy}, and N_{yy}) and moments (M_{xx}, M_{xy}, and M_{yy}) are derived from Hamilton's principle, as shown in Eqs. (10a–10c).

$$\delta\int_{t_0}^{t_1}(U - T - E)dt = 0, \tag{9}$$

$$N_{xx,x} + N_{xy,x} = (\rho_{FRP}h_{FRP} + \rho_c h_c)\ddot{u}_0, \tag{10a}$$

$$N_{yy,y} + N_{xy,y} = (\rho_{FRP}h_{FRP} + \rho_c h_c)\ddot{v}_0, \tag{10b}$$

$$\begin{aligned}&-M_{xx,xx} - 2M_{xy,xy} - M_{yy,yy} - (\rho_{FRP}h_{FRP} + \rho_c h_c)\ddot{w}_0\\ &= P_r\left(1 - \frac{t - t_a}{t_o}\right)\mathrm{e}^{-b\left(1-\frac{t-t_a}{t_o}\right)},\end{aligned} \tag{10c}$$

where, $\ddot{u}_0$, $\ddot{v}_0$, and $\ddot{w}_0$ are $\frac{d^2u_0}{dt^2}$, $\frac{d^2v_0}{dt^2}$, and $\frac{d^2w_0}{dt^2}$, respectively.

The stiffness of concrete has been considered by breaking it into two isotropic layers and including these concrete layers in the laminate configuration. Subsequently, the

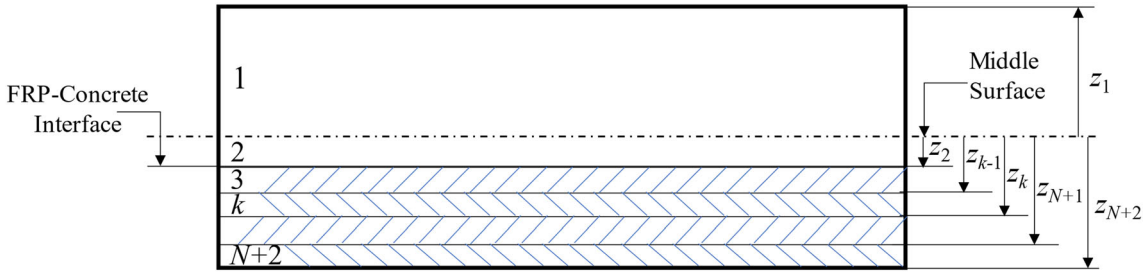

Figure 1. The geometry of concrete wall with *N*-layered FRP laminate on back-face.

resultant stresses and moments are obtained in terms of extensional stiffnesses (A_{ij}), bending-extension coupling stiffnesses (B_{ij}), and bending stiffnesses (D_{ij}), as shown in Eqs. (11a), (11b). The stiffnesses are calculated using Eqs. (12a)-(12c).

$$\begin{Bmatrix} N_{xx} \\ N_{yy} \\ N_{xy} \end{Bmatrix} = \begin{bmatrix} A_{11} & A_{12} & A_{16} \\ A_{12} & A_{22} & A_{26} \\ A_{16} & A_{26} & A_{66} \end{bmatrix} \begin{Bmatrix} \varepsilon_{0xx} \\ \varepsilon_{0yy} \\ \gamma_{0xy} \end{Bmatrix} + \begin{bmatrix} B_{11} & B_{12} & B_{16} \\ B_{12} & B_{22} & B_{26} \\ B_{16} & B_{26} & B_{66} \end{bmatrix} \begin{Bmatrix} \kappa_{xx} \\ \kappa_{yy} \\ \kappa_{xy} \end{Bmatrix}, \tag{11a}$$

$$\begin{Bmatrix} M_{xx} \\ M_{yy} \\ M_{xy} \end{Bmatrix} = \begin{bmatrix} B_{11} & B_{12} & B_{16} \\ B_{12} & B_{22} & B_{26} \\ B_{16} & B_{26} & B_{66} \end{bmatrix} \begin{Bmatrix} \varepsilon_{0xx} \\ \varepsilon_{0yy} \\ \gamma_{0xy} \end{Bmatrix} + \begin{bmatrix} D_{11} & D_{12} & D_{16} \\ D_{12} & D_{22} & D_{26} \\ D_{16} & D_{26} & D_{66} \end{bmatrix} \begin{Bmatrix} \kappa_{xx} \\ \kappa_{yy} \\ \kappa_{xy} \end{Bmatrix}, \tag{11b}$$

$$A_{ij} = \sum_{k=1}^{2} \left(Q_{ij}^{c}\right)_k (z_k - z_{k-1}) + \sum_{k=3}^{N+2} (\overline{Q}_{ij})_k (z_k - z_{k-1}), \tag{12a}$$

$$B_{ij} = \frac{1}{2} \sum_{k=1}^{2} \left(Q_{\mathrm{ij}}^{c}\right)_k (z_k^2 - z_{k-1}^2) + \frac{1}{2} \sum_{k=3}^{N+2} (\overline{Q}_{ij})_k (z_k^2 - z_{k-1}^2), \tag{12b}$$

$$D_{ij} = \frac{1}{3} \sum_{k=1}^{2} \left(Q_{ij}^{c}\right)_k (z_k^3 - z_{k-1}^3) + \frac{1}{3} \sum_{k=3}^{N+2} (\overline{Q}_{ij})_k (z_k^3 - z_{k-1}^3), \tag{12c}$$

where, N is the number of layers in the FRP composite, k implies the k^{th} layer of the laminate configuration, and z_k and $z_{k\text{-}1}$ are defined as shown in figure 1.

The equilibrium relations in terms of displacements are obtained by combining the constitutive relations with Eqs. (10a)-(10c) and (11a), (11b). The equilibrium relations in terms of displacement are expressed in Eqs. (13a)-(13c),

$$\begin{aligned} &A_{11}u_{0,xx} + 2A_{16}u_{0,xy} + A_{66}u_{0,yy} + A_{16}v_{0,xx} \\ &\quad + (A_{12} + A_{66})v_{0,xy} + A_{26}v_{0,yy} \\ &\quad - \left(B_{11}w_{0,xxx} + 3B_{16}w_{0,xxy}\right. \\ &\quad \left. + (B_{12} + 2B_{66})w_{0,xyy} + B_{26}w_{0,yyy}\right) \\ &\quad = (\rho_{FRP}h_{FRP} + \rho_c h_c)\ddot{u}_0, \end{aligned} \tag{13a}$$

$$\begin{aligned} &A_{16}u_{0,xx} + (A_{12} + A_{66})u_{0,xy} + A_{26}u_{0,yy} + A_{66}v_{0,xx} \\ &\quad + 2A_{26}v_{0,xy} + A_{22}v_{0,yy} \\ &\quad - \left(B_{16}w_{0,xxx} + (B_{12} + 2B_{66})w_{0,xxy}\right. \\ &\quad \left. + 3B_{26}w_{0,xyy} + B_{22}w_{0,yyy}\right) \\ &\quad = (\rho_{FRP}h_{FRP} + \rho_c h_c)\ddot{v}_0, \end{aligned} \tag{13b}$$

$$\begin{aligned} &-\left(B_{11}u_{0,xxx} + 2B_{16}u_{0,xxy} + (B_{12} + B_{66})u_{0,xyy}\right. \\ &+ B_{26}u_{0,yyy} + B_{16}v_{0,xxx} + (B_{12} + B_{66})v_{0,xxy} + 2B_{26}v_{0,xyy} \\ &+ B_{22}v_{0,yyy}\left(D_{11}w_{0,xxxx} + 3D_{16}w_{0,xxxy} + 2(D_{12} + D_{66})w_{0,xxyy}\right. \\ &\left.\left. + 3D_{26}w_{0,xyyy} + D_{22}w_{0,yyyy}\right)\right) - (\rho_{FRP}h_{FRP} + \rho_c h_c)\ddot{w}_0 \\ &= P_r\left(1 - \frac{t - t_a}{t_o}\right)\mathrm{e}^{-b\left(1 - \frac{t - t_a}{t_o}\right)}. \end{aligned} \tag{13c}$$

The displacements are assumed to vary as in Eqs. (14a)-(14c), with respect to time across the simply supported wall, considering the center of the wall as the origin,

$$u_0 = \sum_{m,n} U_{mn}(t) \cos \alpha_m x \sin \beta_n y, \tag{14a}$$

$$v_0 = \sum_{m,n} V_{mn}(t) \sin \alpha_m x \cos \beta_n y, \tag{14b}$$

$$w_0 = \sum_{m,n} W_{mn}(t) \cos \alpha_m x \cos \beta_n y, \tag{14c}$$

where, $U_{mn}(t)$, $V_{mn}(t)$, and $W_{mn}(t)$ are the response of the wall in x, y, and z directions, respectively, at time t after detonation of the explosive. The constants α_m and β_n are expressed as in Equations (15a), (15b),

Table 1. Properties of concrete wall.

Density (kg/m^3)	Modulus of elasticity (MPa)	Poisson's ratio
2400	23900	0.2

Table 2. Elastic properties of FRP.

Properties	CFRP	GFRP	AFRP/ KFRP
Density (kg/m^3)	1560	1850	1400
Longitudinal elastic modulus, E_1 (GPa)	130	46	75
Transverse elastic modulus, E_2 (GPa)	8	8.7	6
In-plane shear modulus, G_{12} (GPa)	4.5	3.2	2
Out-of-plane shear modulus, G_{23} (GPa)	3.6	3.2	1
Poisson's ratio, υ_{12}	0.28	0.28	0.34

$$\alpha_m = \frac{m\pi}{a}. \tag{15a}$$

$$\beta_n = \frac{n\pi}{b}. \tag{15b}$$

where, a is the width of the wall in meters, b is the height of the wall in meters, and m and n are the number of half sine waves in x and y-directions, respectively.

The equilibrium relation for the first mode in terms of center node displacement (W_{11}) is simplified to Eq. (16),

$$\begin{aligned}&(\rho_{\mathrm{FRP}}h_{\mathrm{FRP}} + \rho_c h_c)\ddot{W}_{11}(t)\\ &\quad + \left(\alpha_1^4 D_{11} + 2\alpha_1^2\beta_1^2(D_{12} + D_{66}) + \beta_1^4 D_{22}\right)W_{11}(t)\\ &= -P_r\left(1 - \frac{t - t_a}{t_o}\right)\mathrm{e}^{-b\left(1-\frac{t-t_a}{t_o}\right)}.\end{aligned} \tag{16}$$

Viscous damping has been introduced in Eq. (16) by assuming the damping ratio (ξ) as 0.5%. Thus, Eq. (17) can be obtained, which represents the dynamic equilibrium equation for the center node of the wall. Equation (17) has been solved using the central difference method and the direct integration method to determine the response of the FRP laminated wall.

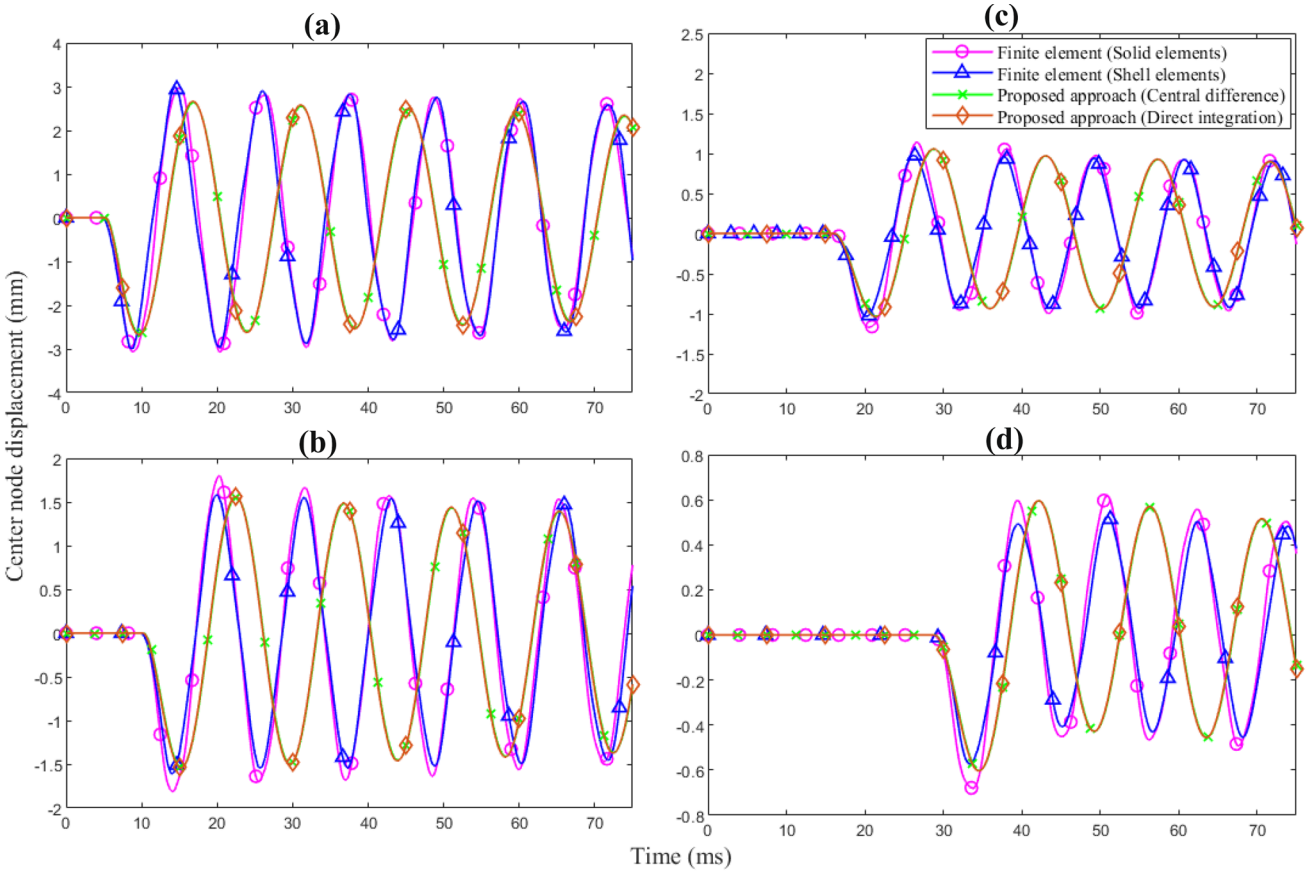

Figure 2. Time-history response of the wall for blast at standoff distance **a** 5 m, **b** 7.5 m, **c** 10 m and **d** 15 m.

Table 3. Effect of standoff distance on blast wave parameters and wall displacement.

	5 m	7.5 m	10 m	15 m
Scaled distance (m/kg$^{1/3}$)	1.357	2.036	2.714	4.072
Peak reflected overpressure (kPa)	2997.04	950.25	422.2	156.39
Arrival time (ms)	3.26	6.72	11.2	22.16
Positive duration (ms)	8.11	7.62	9.5	12.73
Maximum deflection (mm)	8.54	5.16	3.29	1.73

$$M\ddot{W}_{11} + C\dot{W}_{11} + KW_{11} = -P_r\left(1 - \frac{t - t_a}{t_o}\right)e^{-b\left(1-\frac{t-t_a}{t_o}\right)}, \tag{17}$$

where, $M = (\rho_{FRP}h_{FRP} + \rho_c h_c)$, $K = \left(\alpha_1^4 D_{11} + 2\alpha_1^2\beta_1^2(D_{12} + D_{66}) + \beta_1^4 D_{22}\right)$, and $C = 2\xi\sqrt{MK}$.

4. Results and discussion

Parametric studies have been conducted for the 12-layer quasi-isotropic ([0°/90°/45°/-45°/0°/90°]$_s$) CFRP laminated concrete wall using the proposed simplified approach for different, (i) standoff distances, (ii) weights of TNT explosive used, (iii) thicknesses of concrete wall, (iv) number of layers of lamina used, (v) stacking sequence used, and (vi) laminate material used. The geometry of concrete wall fixed with *N*-layered FRP laminate is considered as per [13]. The properties of concrete and FRP used in this study are given in Tables 1 and 2, respectively.

To validate the results obtained by present analytical formulations for the linear dynamic response of the laminated wall, the transverse center node displacement response of a concrete wall laminated with a 12-layer quasi-isotropic CFRP laminate subjected to a blast load generated due to 10 kg TNT explosion is obtained and compared with three-dimensional finite element analysis on commercially available finite element (FE) software, Abaqus/CAE 2020 [14]. The results are found in good agreement, as observed in Figure 2, and therefore the present approach is considered acceptable for preliminary analysis.

4.1 *Variation in standoff distance*

The maximum displacements of the center node are found for four different standoff distances (5 m, 7.5 m, 10 m, and 15 m) for a 50 kg TNT blast, as shown in table 3. The displacements decrease with an increase in the standoff distance, which is expected. The arrival time of the blast can also be seen to increase with an increase in the standoff distance, as given in table 3. At lower standoff distances, it is also observed that the decay in peak overpressure is rapid as compared to the higher standoff distances.

As the standoff distance increases, the scaled distance also increases, which mandates recalculating blast load parameters. As per the Kingery-Bulmash plots, the increase in scaled distance is accompanied by an increase in arrival time and a decrease in peak overpressure, which is in line with the observation. This decrease in peak overpressure reduces the loading on the concrete wall with the FRP laminates, leading to lower displacements of the wall.

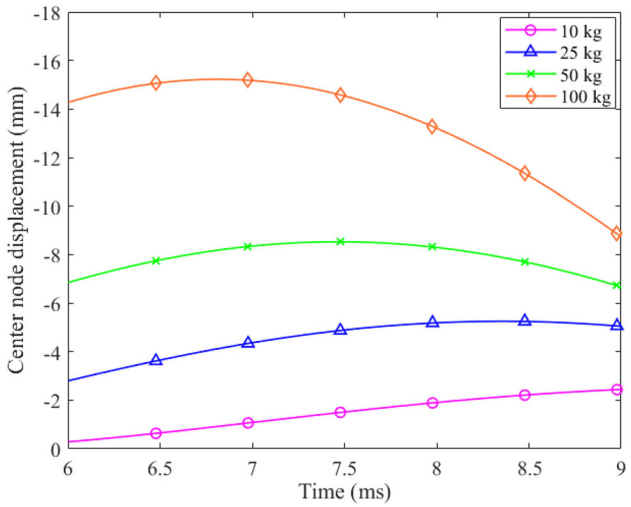

Figure 3. Effect of weight of explosive on center node displacement of the wall.

4.2 *Variation in explosive charge weight*

The displacement response of the center node of the concrete wall with the FRP laminates for four different explosive charge weights of 10 kg, 25 kg, 50 kg, and 100 kg at a standoff distance of 5 m for a 200 mm thick concrete wall is shown in figure 3. The deflection caused due to a 10 kg blast event is 50% lower, a 50 kg blast event is 62% higher, and a 100 kg blast event is 190% higher than those due to a 25 kg blast event. The displacements obtained are observed to increase with an increase in the charge weight. This increase can be attributed to a decrease

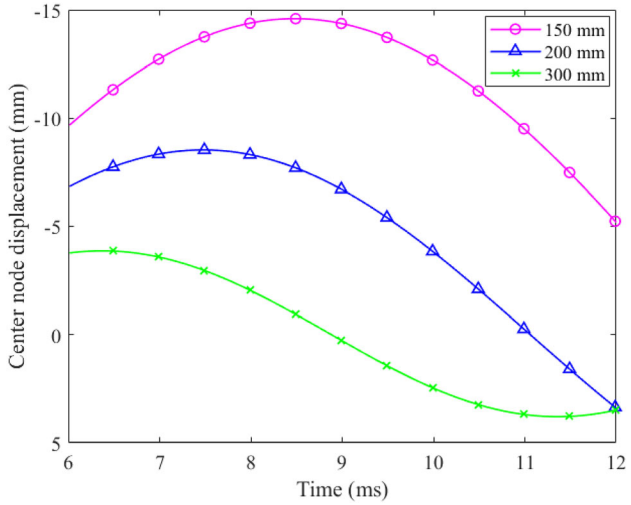

Figure 4. Effect of thickness of the concrete wall on center node displacement of the wall.

in the scaled distance, which causes an increase in the pressure loads on the wall, leading to higher displacements.

4.3 *Variation in concrete wall thickness*

The center node displacements of an FRP laminate on a concrete wall with wall thickness of 150 mm, 200 mm, and 300 mm for 50 kg TNT charge weight kept at a 5 m standoff distance are shown in figure 4. The displacement is observed to be the highest for a 150 mm thick concrete wall, which can be associated with higher damage. It is also observed that the displacement decreases as the thickness of the concrete wall increases, which is expected. The displacement for a 200 mm thick concrete wall is 41% less, and that of a 300 mm thick concrete wall is 73.5% less as compared to a 150 mm thick concrete wall.

The increase in thickness of the concrete wall leads to an obvious increase in the stiffness of the wall, thus providing higher resistance to displacements caused due to blast loads. Moreover, the mass of the wall increases with an increase in the thickness of the concrete wall, which also increases the overall damping capacity of the structure. Thus, the decrease in displacement due to an increase in the thickness of the concrete wall can be attributed to an increase in both the stiffness and the mass of the wall, which is expected.

4.4 *Variation in laminate layers and stacking sequence*

Figures 5(a) and (b) show the effect of the number of layers of lamina and their stacking sequence on the dynamic displacement response of the wall, respectively. As expected, the displacement is observed to be higher when the laminate consists of a lower number of layers due to a reduction in stiffness. The center node displacement when a 12-layer angle ply laminate is used is around 15% lower, and when an 8-layer angle ply laminate is used, it is almost 8% lower when compared to a 4-layer angle ply laminate.

The displacement is calculated for four different symmetric laminate orientations $[0°/90°/45°/-45°/0°/90°]_s$, $[0°/45°/-45°/90°/0°/45°]_s$, $[0°/90°/0°/90°/0°/90°]_s$, and $[45°/-45°/45°/-45°/45°/-45°]_s$. It is observed that the

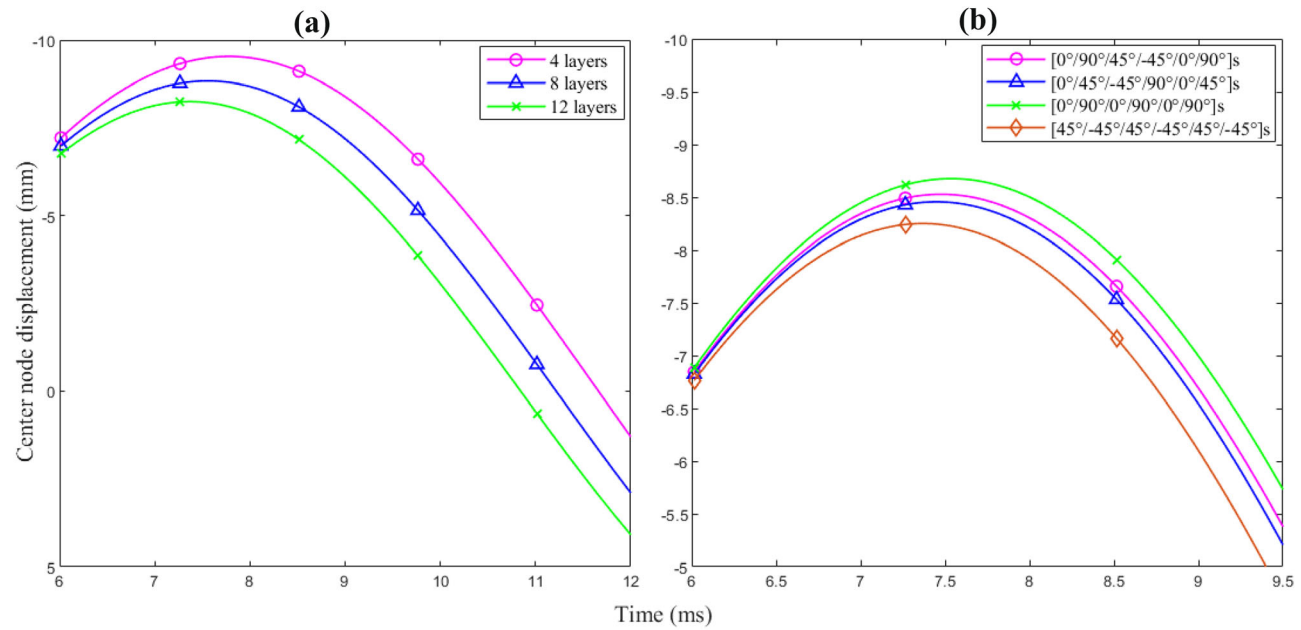

Figure 5. Effect of **a** number of lamina layers in angle ply laminate $[45°/-45°/45°/-45°/45°/-45°]_s$ and **b** the stacking sequence on center node displacement of the wall.

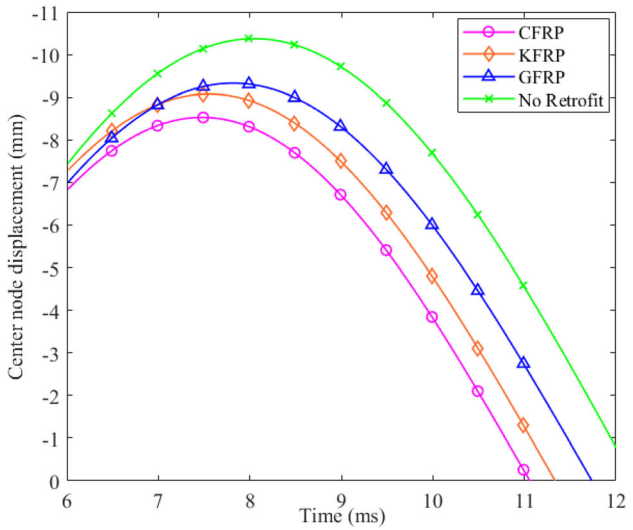

Figure 6. Efficacy of different laminates for reduction of center node displacement of the wall.

cross-ply laminate ($[0°/90°/0°/90°/0°/90°]_s$) shows the highest deflection among the considered configurations here. The angle ply laminate ($[45°/-45°/45°/-45°/45°/-45°]_s$) shows the lowest displacement, which is 5% lower than the displacement shown by cross-ply laminate. The stacking sequence of a laminate influences the stiffness of the laminate. Thus, the difference in the dynamic response can be associated with a change in the stiffness of the laminate due to the stacking sequence. However, in this case, a higher response cannot necessarily be attributed to higher damage as some stacking sequences might lead to debonding failure earlier than others, irrespective of the difference in response.

4.5 *Variation in FRP material*

Figure 6 shows the displacement response of the laminated wall subjected to a 50 kg TNT explosion at a standoff distance of 5 m when CFRP, GFRP, and Aramid FRP (AFRP or KFRP) laminates are used. Their displacement response is also compared with the displacement obtained when no FRP laminate is used to study the efficacy of using FRP laminates. It is observed that a CFRP laminate reduces the response of a bare concrete wall by almost 18%, GFRP reduces the response by around 10%, and AFRP reduces the response by around 13%. This demonstrates that the high stiffness of FRP leads to lower displacement of the wall, hence governs the design.

5. Conclusions

A simply supported concrete wall laminated with a symmetric fiber-reinforced polymer laminate subjected to blast-induced loads is analyzed using the proposed simplified approach in this study. Inhouse MATLAB codes are developed to determine the blast loading and the center node displacement response of the wall. Several parameters, such as the weight of explosives, type of explosives, property of laminae, orientation of laminae, and the standoff distance, are considered for conducting a preliminary analysis using the proposed analytical approach. The proposed approach has further been used to conduct a parametric sensitivity study for different (i) standoff distance, (ii) weight of TNT explosive used, (iii) thickness of concrete wall, (iv) number of layers of lamina used, (v) stacking sequence used, and (vi) laminate materials. The following conclusions are arrived at from the present study: i. The displacement response obtained through the proposed approach to conduct a preliminary analysis of an FRP laminate on a concrete wall subjected to blast loads shows excellent agreement with the finite element analysis results and agrees with the consensus, validating this method's accuracy. Thus, further conclusions are drawn using the results obtained through the proposed analytical approach. ii. Higher standoff distances reduce the blast load and displacements of the wall significantly. Thus, higher standoff should be provided with the help of physical barriers or by creating restricted zones near high-risk areas, as part of perimeter protection. This approach might prove economical than strengthening and therefore consider viable. iii. The displacements are observed to increase with an increase in charge weights. The displacements for a 100 kg TNT blast are 190% higher, and for a 50 kg TNT blast, are 62% higher than those due to a 25 kg blast. iv. The displacements as reduced drastically for thick concrete walls; as compared to 150 mm thick concrete walls, 300 mm and 200 mm thick concrete walls show a reduction of 73.5% and 41% in center node displacements, respectively. Thus, in situations where a thick concrete wall is possible to provide, the need for FRP laminates can be reassessed, and the less expensive mitigation strategy of thickening can be used instead, at the expense of larger footprint. v. The displacements are observed to increase with a decrease in the number of layers in the FRP laminate. Thus, the number of layers should be decided by optimizing the cost and the performance requirements of the structure. vi. The stacking sequence and ply orientation also affect the response of the concrete wall with the FRP laminates. The angle-ply laminates show the lowest displacement, while the cross-ply laminates show the highest response amongst the considered laminates. Thus, it is necessary to check for the best possible stacking sequence and ply orientation in the design. vii. Among the FRP composite materials studied, the CFRP reduces the response of a concrete wall by 18%, GFRP reduces the response by 10%, and AFRP reduces the response by 13%. Thus, using FRP laminates helping to reduce the deflection of concrete walls, which may also help in reducing the damage. Moreover, it is important to choose the optimum FRP material considering their cost and performance requirements.

List of symbols

u, v, w	Displacements of a point on the wall along the x, y, and z directions, respectively
u_0, v_0, w_0	Midplane displacements of the wall along the x, y, and z directions, respectively
ε, γ	Membrane and shear strains, respectively
σ, τ	Normal and shear stress, respectively
ε_0, $\gamma 0$, κ	Midplane membrane, shear, and curvature strains, respectively
ρ_{FRP}, ρ_c	Density of FRP and concrete, respectively
h_{FRP}, h_c	Thickness of FRP laminate and concrete wall, respectively
M, K, C	Mass, stiffness, and damping coefficient of the wall, respectively
P_{so}, P_r	Incident and reflected overpressure due to the blast wave, respectively
P_o	Ambient pressure
t, t_a, t_o	Time after the blast, arrival time of the blast wave, and positive duration, respectively
R	Distance of the concerned point from the point of explosion
We, W_{Exp}	Equivalent TNT weight and actual weight of an explosive, respectively
H^d_{exp}, H^d_{TNT}	Heat of detonation of explosive and heat of detonation of TNT, respectively
Z	Scaled distance
Q^c_{ij}, Q_{ij}, $\overline{Q}_{ij}$	Reduced stiffness of concrete, reduced stiffness of FRP lamina, and transformed reduced stiffness of FRP lamina, respectively

Acknowledgement

The authors are grateful to the Aeronautics Research and Development Board (AR&DB), Defence Research and Development Organization (DRDO) for extending funding to carry out this research work through a project titled, “Development of Functionally Graded Hybrid Fiber Reinforced Polymer Composites for High Strain Rate and Elevated Temperature Aeronautical Application”, sanctioned under grant-in-aid scheme. The opinions expressed in the article are those of the authors and not that of the funding agency.

References

[1] Ross C A, Purcell M R and Jerome E L 1997 Blast response of concrete beams and slabs externally reinforced with fiber reinforced plastics (FRP). American Society of Civil Engineers (ASCE), Building to Last, pp 673–677

[2] Muszynski L C and Purcell M R 2003 Composite reinforcement to strengthen existing concrete structures against air blast. *J. Compos. Construct.* 7(2): 93–97

[3] Muszynski L C and Purcell M R 2003 Use of composite reinforcement to strengthen concrete and air-entrained concrete masonry walls against air blast. *J. Compos. Construct.* 7(2): 98–108

[4] Jain S, Tiwari R, Chakraborty T and Matsagar V 2015 Dynamic response of reinforced concrete wall under blast loading. *Indian Concr. J.* 89(8): 27–41

[5] Maazoun A, Matthys S, Atoui O, Belkassem B and Lecompte D 2022 Finite element modelling of RC slabs retrofitted with CFRP strips under blast loading. *Eng. Struct.* 252: 113597

[6] Kingery C N and Bulmash G 1984. Airblast parameters from TNT spherical air burst and hemispherical surface burst. Technical Report ARBRLTR02555, US Army armament research and development center, ballistics research laboratory, Aberdeen Proving Ground, Maryland (MD), USA

[7] Goel M, Matsagar V, Marburg S and Gupta A 2012 An abridged review of blast wave parameters. *Defence Sci. J.* 62(5): 300–306

[8] Birman V and Bert C W 1987 Behaviour of laminated plates subjected to conventional blast. *Int. J. Impact Eng.* 6(3): 145–155

[9] Goel M D, Matsagar V A and Gupta A K 2011 Dynamic response of stiffened plates under air blast. *Int. J. Protect. Struct.* 2(1): 139–155

[10] Karlos V and Solomos G 2013. Calculation of blast loads for application to structural components. Administrative Arrangement No JRC 32253-2011 with DG-HOME Activity A5 - Blast simulation technology development. EUR 26456. Luxembourg (Luxembourg): Publications Office of the European Union. JRC87200

[11] Karlos V, Solomos G and Larcher M 2016 Analysis of the blast wave decay coefficient using the Kingery-Bulmash data. *Int. J. Protect. Struct.* 7(3): 409–429

[12] MATLAB release, 2022 2022. The MathWorks Inc, Natick, Massachusetts (MA), USA

[13] Jones R M 1998. *Mechanics of Composite Materials*. CRC Press, Taylor & Fracis Group

[14] Abaqus/Standard User’s Manual 2020. Dassault Systèmes Simulia Corporation, Providence, Rhode Island (RI), USA